Available online at www.sciencedirect.com
SCIENCE DIRECT®
Pattern Recognition Letters 27 (2006) 1478–1486
Pattern Recognition Letters
www.elsevier.com/locate/patrec

Personal authentication using hand images ☆

Ajay Kumar [a,b,*], David C.M. Wong [b], Helen C. Shen [b], Anil K. Jain [c]

[a] Department of Electrical Engineering, Indian Institute of Technology Delhi, Hauz Khas, New Delhi, India
[b] Department of Computer Science, Hong Kong University of Science and Technology, Clear Water Bay, Hong Kong
[c] Pattern Recognition and Image Processing Lab, Department of Computer Science and Engineering, Michigan State University, East Lansing, MI 48824, United States

Received 14 September 2004; received in revised form 14 December 2005
Available online 19 May 2006

Communicated by Prof. H. Kim

Abstract

This paper presents a new approach for personal authentication using hand images. The proposed method attempts to improve the performance of palmprint-based verification system by integrating hand geometry features. Unlike prior bimodal biometric systems, the users do not have to undergo the inconvenience of using two different sensors in our system since the palmprint and hand geometry images are acquired simultaneously using a single camera. The palmprint and handshape images are used to extract salient features and are then examined for their individual and combined verification performances. The image acquisition setup used here is inherently simple and it does not employ any special illumination nor does it use any alignment pegs to cause any inconvenience to the users. Our experiments on an image database of 100 users achieve promising results and suggest that the fusion of matching scores can achieve better performance than the fusion at representation.

Keywords: Hand verification; Palmprint verification; Hand geometry; Information fusion

1. Introduction

Reliability in personal authentication is key to the stringent security requirements in many application domains ranging from airport surveillance to electronic banking. Many physiological characteristics of humans, i.e., biometrics, are typically invariant over time, easy to acquire, and unique to each individual. Biometric features such as face, iris, fingerprint, hand geometry, palmprint, signature, etc. have been suggested for enhanced security in access control. Most of the current research in biometrics is focused on fingerprint and face (Jain et al., 1999). The reliability of personal identification using face is currently low as the available commercial systems continue to grapple with the problems of pose, lighting and expression (Yang et al., 2002). Personal authentication using fingerprints has shown to work well in most cases. However, a large segment of users, such as elderly people and manual laborers, fail to deliver good quality fingerprints/minutiae and, therefore, the usage of fingerprint based techniques has some limitations. The surface area of fingerprints is quite small and any cuts or scar mark on this surface generates false minutiae, which undermines the integrity of the system. As a result, other biometric characteristics are receiving increasing attention. Moreover, additional biometric features, such as palmprints, can be easily integrated with the existing fingerprint based and/or hand shape based

☆ A preliminary version of this paper was orally presented in 4th *Internat. Conf. on Audio Video based Biometric Personal Authentication*, Guildford (UK), June 9–11 2003.

* Corresponding author. Address: Department of Computing, The Hong Kong Polytechnic University, PQ-711, Hung Hom, Kowloon, Hong Kong. Tel.: +852 2766 7288; fax: +852 2774 0842.
E-mail addresses: ajaykr@ieee.org (A. Kumar), csdavid@cs.ust.hk (D.C.M. Wong), helens@cs.ust.hk (H.C. Shen), jain@cse.msu.edu (A.K. Jain).

0167-8655/$ - see front matter © 2006 Published by Elsevier B.V.
doi:10.1016/j.patrec.2006.02.021

authentication systems to provide enhanced level of confidence in personal authentication.

1.1. Prior work

Two kinds of biometric indicators can be extracted from the low-resolution[1] hand images; (i) palmprint features, which are composed of principal lines, wrinkles, minutiae, delta points, etc., and (ii) hand geometry features which include area/size of palm and length and width of fingers. The problem of personal authentication using palmprint features has drawn considerable attention and researchers have proposed various methods (Kumar and Shen, 2002, 2004; Li et al., 2002; You et al., 2002; Wu et al., 2002; Zhang and Shu, 1999; Kumar and Zhang, 2005; Duta et al., 2002; Funada et al., 1998; Chen et al., 2001; Joshi et al., 1998; Kung et al., 1995; Han et al., 2003). One popular approach considers palmprints as textured images which are claimed to be unique to every individual. Therefore, analysis of palmprint images using Gabor filters (Kumar and Shen, 2004), wavelets (Kumar and Shen, 2002), Fourier transform (Li et al., 2002), and local texture energy (You et al., 2002) has been proposed in the literature. Palmprints have a large number of creases and Wu et al. (2002) have characterized these creases by directional line energy features and used them for palmprint identification. The endpoints of some prominent principal lines, i.e., the heart-line, head-line, and life-line are rotation invariant. Some authors (Zhang and Shu, 1999) have used these endpoints and midpoints for the registration of geometrical and structural features of principal lines for palmprint matching. Kumar and Zhang (2005) have recently proposed the simultaneous usage of multiple palmprint representations to achieve reliable authentication. Duta et al. (2002) have suggested that the connectivity of extracted palm lines is not important. Therefore, they have used a set of feature points along the prominent palm lines, instead of extracted palm lines as in (Zhang and Shu, 1999), to generate the matching score for palmprint authentication. The palmprint pattern also contains ridges and minutiae, similar to a fingerprint pattern. However, in palmprints the creases and ridges often overlap and cross each other. Therefore, Funada et al. (1998) have suggested the extraction of local palmprint features, i.e., ridges, by eliminating the creases. However, this work (Funada et al., 1998) is only limited to the extraction of ridges, and does not go beyond its usage to support the success of these extracted ridges in the identification of palmprints. Chen et al. (2001) have attempted to estimate palmprint crease points by generating a local gray level directional map. These crease points are connected together to isolate the crease in the form of line segments, which are used in the matching process. No details are provided in (Chen et al., 2001) to suggest the robustness of these partially extracted creases for the matching of palmprints. Some related work on palmprint verification also appears in (Joshi et al., 1998; Kung et al., 1995). Han et al. (2003) use morphological and Sobel edge features to characterize palmprints and trained a neural network classifier for their verification.

The palmprint authentication methods in (You et al., 2002; Zhang and Shu, 1999; Duta et al., 2002; Funada et al., 1998; Chen et al., 2001) utilize inked palmprint images while the recent work in (Kumar and Shen, 2002; Han et al., 2003) has shown the utility of inkless palmprint images acquired from the digital scanner. However, some promising results on palmprint images acquired from image acquisition systems using CCD based digital camera appear in (Kumar and Shen, 2004; Li et al., 2002; Kumar and Zhang, 2005).

The US patent office has issued several patents (Sidlauskas, 1988; Jacoby et al., 1972; Miller, 1971; Ernst, 1971) for devices that measure hand geometry features for personal verification. Han et al. (2002) describe a device and system for personal authentication using bootstrap technique which effectively utilizes hand geometry features. A recent European patent (Gunther, 2002) discloses a similar system using hand geometry features. Some related work using low-resolution digital hand images appears in (Sanchez-Reillo et al., 2000; Jain et al., 1999; Oden et al., 2003). These authors have used fixation pegs to restrict the hand movement and shown promising results. However, the results in (Sanchez-Reillo et al., 2000; Jain et al., 1999; Oden et al., 2003) may be biased by the small size of the database and an imposter can easily violate the integrity of system by using fake hand.

1.2. Proposed system

The palmprint and hand geometry images can be extracted from a hand image in a single shot at the same time. Unlike other multibiometrics systems (e.g., face and fingerprint (Hong and Jain, 1998), voice and face (Ben-Yacoub et al., 1999), etc.), a user does not have to undergo the inconvenience of passing through multiple sensors. Furthermore, the fraud associated with fake hand, in hand geometry based verification system, can be checked with the integration of palmprint features. This paper (Kumar et al., 2003) presents a new method of personal authentication using palmprint and hand geometry features that are simultaneously acquired from a single hand image.

The block diagram of the proposed authentication system is shown in Fig. 1. The gray level hand images of every user are acquired from a digital camera and used to automatically extract the palmprint and hand geometry features. These images are first binarized using global thresholding. The resultant binary image is used to estimate the orientation of hand since in the absence of pegs, users do not necessarily align their hand in a preferred direction. The rotated binary image is used to compute

[1] High resolution hand images, of the order of 500 dpi, can also be used to extract fingerprint features. However, the database for such images will require large storage and computational requirements.

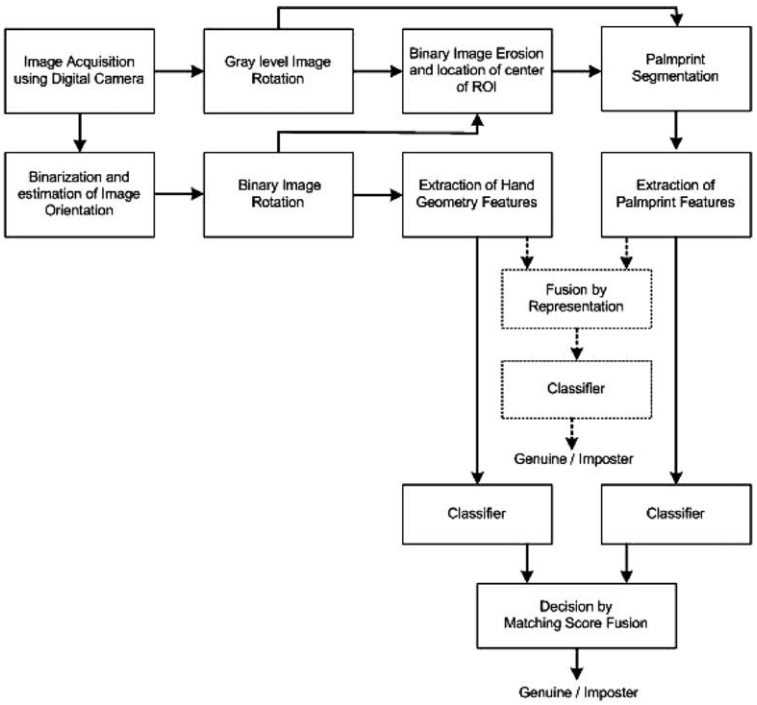

Fig. 1. Block diagram of the Personal Authentication System using hand images.

hand geometry features. This image also serves to estimate the center of palmprint using morphological operations. The estimated center point is used to extract the palmprint image, i.e. a region of interest of a fixed size from the rotated gray level hand images. Each of these palmprint images are used to extract significant local features. Thus, the palmprint and hand geometry features of an individual are obtained from the same hand image. As shown in Fig. 1, two schemes for the fusion of features, fusion at the matching score level and at the representation level, were considered. The matching score level fusion gave better results as discussed in Section 5.

2. Image acquisition and alignment

Our image acquisition setup is inherently simple and does not employ any special illumination (as in Kumar and Shen, 2004) nor does it use any pegs to cause any inconvenience to users (as in Sanchez-Reillo et al., 2000). An Olympus C-3020 digital camera, with 1280×960 pixel resolution, was used to acquire the hand images. Fig. 2 shows a typical acquisition of hand images using our set up. The camera was used in auto focus mode with its optical axis aligned with the region of interest. The illumination of hand images was mainly due to fluorescent lights in indoor lab environment, which was fairly stable during the period of data collection. The image data was collected over a period of three months from the users in the age group of 16–50 years. During image acquisition, the users were only requested to make sure that (i) their fingers do not touch each other and (ii) most of their hand (back side) touches the imaging table.

Fig. 2. Acquisition of a typical hand image using digital camera, with our simple setup.

2.1. Extraction of hand geometry images

The hand geometry features can be easily and efficiently computed from the binary image depicting only the hand shape. Therefore, the acquired hand images are first binarized using image thresholding. Otsu's method of optimal threshold selection (Otsu, 1978) is used. Since the image background is stable (black) and lighting conditions during image acquisition remain relatively constant, the threshold

value can be computed once and used subsequently for other images. Each of the binarized images has to be aligned in a preferred direction so as to capture the same features for matching. The binarized shape of the hand can be approximated by an ellipse. The parameters of the best-fitting ellipse, for a given binary hand shape, are computed using the moments (Baskan et al., 2002). Let $I(x,y)$ denote the pixel value of binary hand shape image S and let (c_x, c_y) denote the location of its centroid. The orientation of image S, i.e., φ, is approximated by counterclockwise orientation of the major axis relative to column axis and is computed as follows (Haralick and Shapiro, 1991):

$$\varphi = \begin{cases} \tan^{-1}\left(\dfrac{m_{02}-m_{20}+\sqrt{(m_{02}-m_{20})^2+4m_{11}^2}}{-2m_{12}}\right) & \text{if } m_{02} > m_{20} \\ \tan^{-1}\left(\dfrac{-2m_{11}}{m_{20}-m_{02}+\sqrt{(m_{20}-m_{02})^2+4m_{11}^2}}\right) & \text{otherwise} \end{cases} \tag{1}$$

where m_{02}, m_{20}, m_{11} are the normalized second-order moments of pixel formation inside the image S, i.e.,

$$m_{02} = \frac{\sum_{(x,y)\in S}(y-c_y)^2 \cdot I(x,y)}{\sum_{(x,y)\in S} I(x,y)}, \quad m_{20} = \frac{\sum_{(x,y)\in S}(x-c_x)^2 \cdot I(x,y)}{\sum_{(x,y)\in S} I(x,y)}$$
$$\text{and } m_{11} = \frac{\sum_{(x,y)\in S}(y-c_y)(x-c_x) \cdot I(x,y)}{\sum_{(x,y)\in S} I(x,y)} \tag{2}$$

The difference between the normal and estimated orientation of image $I(x,y)$, i.e. φ, is the required angle of rotation. The steps of this process can also be seen in Fig. 3. The estimated orientation of binarized image is also used to rotate gray-level hand image, from which the palmprint image is extracted as detailed in the next subsection.

2.2. Extraction of palmprint images

The extraction of region of interest, i.e., palmprint image containing palm-lines and creases, is necessary to extract palmprint features. The location of the center of palmprint images is estimated from the hand geometry images extracted in Section 2.1. Each of these binary images is subjected to morphological erosion, with a known binary structuring element (SE). Let R be the set of non-zero pixels in the binary hand geometry image and SE be the set of non-zero pixels, i.e., structuring element. The morphological erosion is performed as follows:

$$R \Theta \mathrm{SE} = \{g : \mathrm{SE}_g \subseteq R\} \tag{3}$$

where SE_g denotes the structuring element with its reference point shifted by g pixels. A square structuring element (SE) is used to probe the composite binarized image. The palmprint area in hand geometry images is not perfectly square. Therefore, depending on the structure and size of SE, after every erosion operation a residue of the binarized image is expected. The center of binary hand image after erosion, i.e., the center of rectangle that can enclose the residue is determined. The coordinates of the center are used to extract the palmprint embedded in hand images.

The alignment of acquired gray-level hand images can be achieved by counterclockwise rotation of these images by φ degrees using the rotation matrix Z, i.e.,

$$Z = \begin{bmatrix} \cos(\varphi) & -\sin(\varphi) \\ \sin(\varphi) & \cos(\varphi) \end{bmatrix} \tag{4}$$

The rotated images can be used to segment (crop) the palmprint images, of a fixed size, centered at the computed center point from the aligned hand geometry image (Fig. 3(e)). Alternatively, the computed center point can be directly used to estimate the palmprint image pixels in acquired gray-level image. The aligned palmprint images can be obtained by multiplying the position vector of these estimated palmprint pixels with rotation matrix Z. The later method of image rotation using estimated palmprint pixels is computationally simple and used in this work.

2.3. Normalization of palmprints

The extracted palmprint images are normalized to have pre-specified mean and variance. The normalization is used to reduce the possible imperfections in the image due to sensor noise and non-uniform illumination. The method for normalization employed here is the same as suggested in (Prabhakar et al., 2003) and is sufficient for the quality

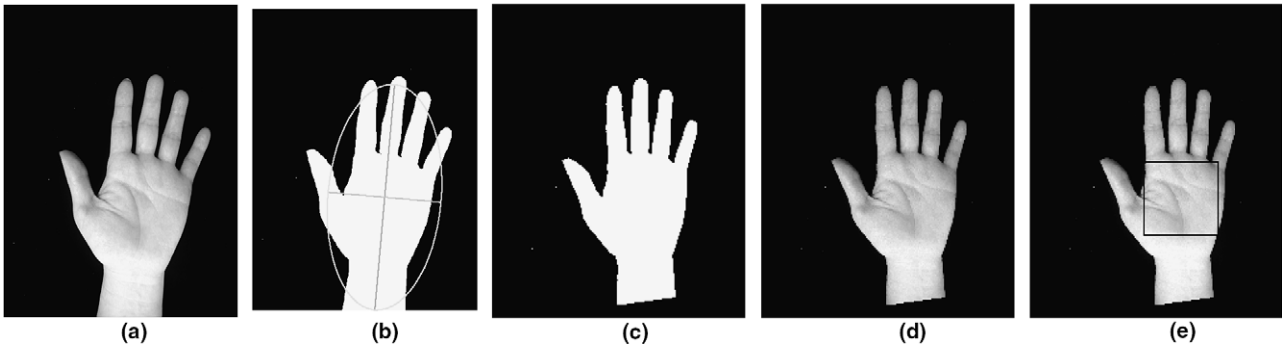

Fig. 3. Extraction of two biometric modalities from the hand image: (a) captured image from the digital camera, (b) binarized image and ellipse fitting to compute the orientation, (c) binary image after rotation, (d) gray scale image after rotation and (e) ROI, i.e. palmprint, obtained from image (d).

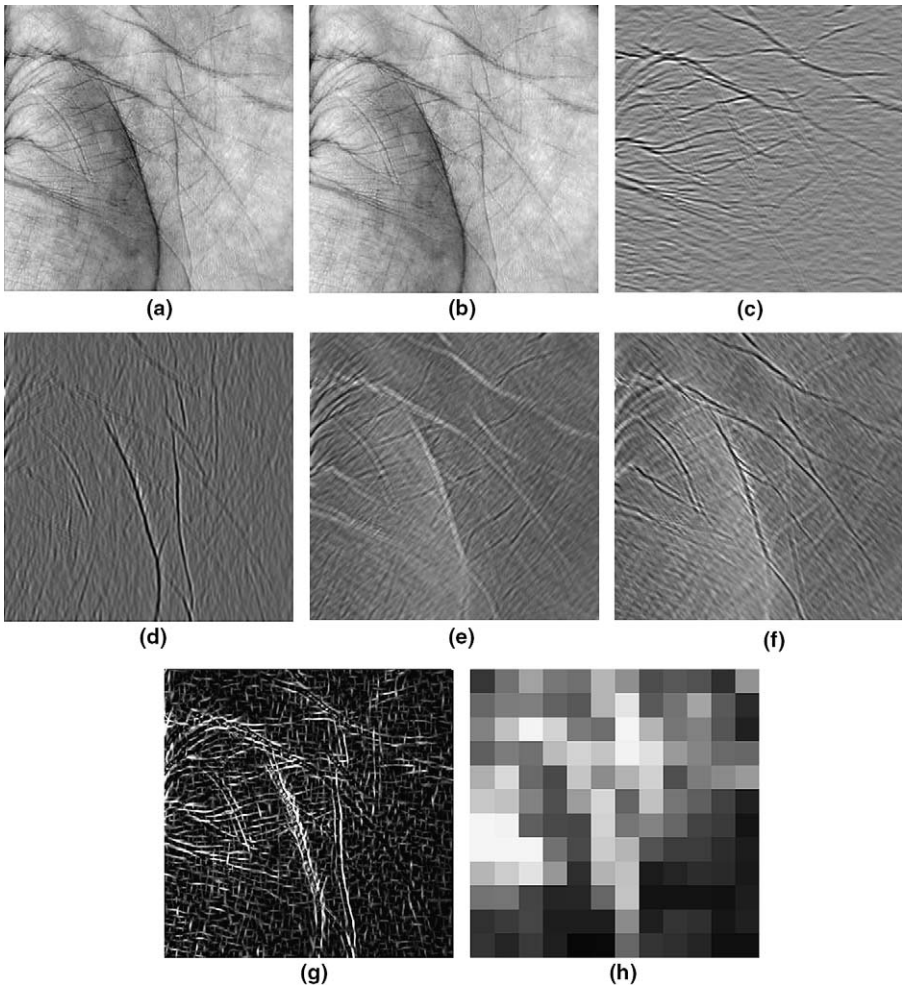

Fig. 4. Palmprint feature extraction: (a) segmented image, (b) image after normalization, filtered images with directional mask at orientation 0° in (c), 90° in (d), 45° in (e), 135° in (f), (g) image after voting, and (h) standard deviation of gray level values from each of the 144 overlapping blocks.

of acquired images in our experiments. Let the gray level at (x,y), in a palmprint image J be represented by $J(x,y)$. The mean and variance of image, M and V respectively, can be computed from the gray levels of the pixels. The normalized image $J'(x,y)$ is computed using the pixel-wise operations as follows:

$$J'(x,y) = \begin{cases} M_{\mathrm{d}} + \lambda & \text{if } J(x,y) > M \\ M_{\mathrm{d}} - \lambda & \text{otherwise} \end{cases} \tag{5}$$

where $\lambda = \sqrt{\frac{V_{\mathrm{d}}\{J(x,y)-M\}^2}{V}}$, M_{d} and V_{d} are the desired values for mean and variance, respectively. These values are pretuned according to the image characteristics, i.e., $J(x,y)$. In all our experiments, the values of M_{d} and V_{d} were fixed to 100. Fig. 4(a) and (b) shows a typical palmprint image before and after the normalization.

3. Feature extraction

3.1. Extraction of palmprint features

The palmprint pattern is mainly made up of palm lines, i.e., principal lines and creases. Line feature matching (Zhang and Shu, 1999; Han et al., 2003) is reported to be powerful and offers high accuracy in palmprint verification. However, it is very difficult to accurately characterize these palm lines, i.e., their magnitude and direction, in noisy images. Therefore, a robust but simple method is used here. Four line detection operators consisting of four convolution masks (Haralick and Shapiro, 1991), tuned to detect lines at a particular orientation, are used to extract significant line features from each of the normalized palmprint images. Each of these masks can detect lines oriented at 0° (h_1), 45° (h_2), 90° (h_3), and 135° (h_4). The spatial extent of these masks was empirically fixed as 9×9. Each of these masks is used to filter the normalized palmprint images as follows:

$$J_1(x,y) = |h_1 * J'(x,y)| \tag{6}$$

where '*' denotes the discrete 2D convolution. Thus four filtered images, i.e., $J_1(x,y)$, $J_2(x,y)$, $J_3(x,y)$ and, from each of the masks h_1, h_2, h_3 and h_4, respectively, are obtained. The gray level pixels from each of these four images are used to generate the final image $J_{\mathrm{f}}(x,y)$ as follows:

$$J_{\mathrm{f}}(x,y) = \max_{(x,y)\in J} \{J_1(x,y), J_2(x,y), J_3(x,y), J_4(x,y)\} \tag{7}$$

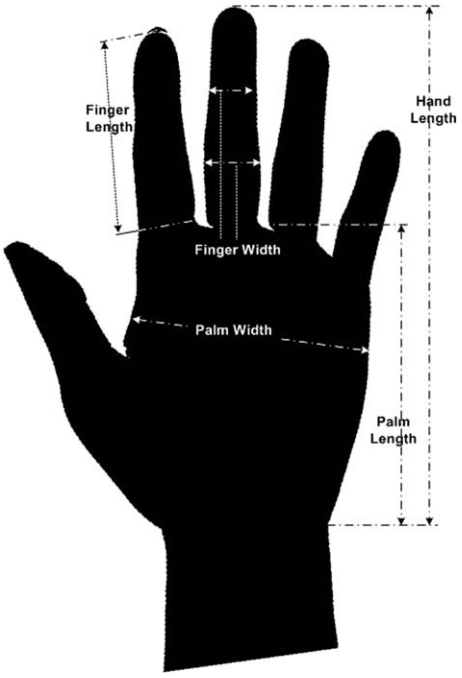

Fig. 5. Hand geometry feature extraction.

The resultant image represents the combined directional map of palm-lines in the palmprint image $J(x,y)$. The image pixels in $J_f(x,y)$ can be efficiently characterized by the localized estimation of statistical moments. For computational reasons, we used standard deviation to compute the localized palmprint features. The image $J_f(x,y)$ is divided into a set of n overlapping blocks and standard deviation of pixels in each of these overlapping blocks is used to form the feature vector.

$$v_{\text{palm}} = \{\sigma_1, \sigma_2, \ldots, \sigma_n\} \tag{8}$$

where σ_1 is the standard deviation in the overlapping first block. The extraction of palmprint features using this method is also shown in Fig. 4. The palmprint images from every user is characterized by feature vector v_{palm} and used for identification.

3.2. Extraction of hand geometry features

The hand geometry features such as length and width of fingers, thickness and relative location of these features, form the second set of discriminant features from the hand images. The binary images[2] such as the one shown in Fig. 3(c), is used to compute significant hand geometry features. A total of 16 hand geometry features were used (Fig. 5); 4 finger lengths, 8 finger widths (2 widths per finger), palm width, palm length, hand area, and hand length. The lengths of fingers are efficiently computed by defining a pair of control points in the binary image. The tip of fingers and the interfinger points, i.e. gap between fingers and finger end points, formed such a pair. The tip of fingers are the positive local extremes of the curvature obtained from first- and second-order moments of the boundary pixels. Similarly, the negative local extremes of the hand boundary constitute the interfinger points. The method of extracting hand geometry features is similar as detailed in (Sanchez-Reillo et al., 2000; Oden et al., 2003). Thus, the geometry of every hand image is characterized by the feature vector v_{hg} of length 1×16.

[2] Due to the usage of palmprints, the palm side of hand images are imaged and used to compute hand geometry features while prior work (Sanchez-Reillo et al., 2000; Jain et al., 1999) uses other side of hand images.

4. Information fusion and matching criterion

The multiple pieces of evidences can be combined by a number of information fusion strategies that have been proposed in the literature (Kittler et al., 1998; Prabhakar and Jain, 2002; Kumar et al., 2003). In the context of biometrics, it has been shown that the trainable fusion strategies do not necessarily offer better performance than simple fusion rules (Kittler and Messer, 2002). The information fusion strategies employed in multimodal biometric systems can be categorized into three levels; (i) fusion at representation level, where the feature vectors of multiple biometric are concatenated to form an augmented feature vector, (ii) fusion at matching score level, where the matching scores of multiple biometric system are combined to generate a final decision score, and (iii) fusion at abstract level, where decision output from multiple biometric systems are consolidated. The first two fusion schemes are more relevant for a bimodal biometric system and were considered in this work. During user authentication, a user is required to claim his/her identity while presenting his hand for imaging. The query feature vector from the user (v_q) is computed with the feature vector for the claimed identity (v_c) that is available from the biometric database. The similarity measure between these two feature vectors is used to compute the matching score.

$$s = \frac{v_q \cdot v_c}{|v_q||v_c|} \tag{9}$$

The similarity measure defined in the above equation computes the normalized correlation between the feature vectors v_q and v_c. If the matching score $s$is less than some prespecified threshold then the user is assumed to be an imposter else we decide him/her as genuine.

The measurement scale for feature vectors from palmprint and hand geometry is different, and their direct concatenation, for fusion at representation, may not offer improved performance. Therefore each of the feature vectors from hand geometry has to be normalized and the range of normalization can be computed from the training samples of the palmprint feature vectors. The normalized feature vectors from the palmprint (v_p) and hand-geometry (v_{hg}) are concatenated to compute the feature vector (v_{cf}) for the combined hand representation, i.e.

$$v_{cf} = [v_p \quad v_{hg}] \tag{10}$$

The similarity scores (9) computed from combined feature vector (10) is used to authenticate users. Another matching score level fusion approach examined in this work computes individual matching scores, i.e. similarity scores s_p and s_{hg} for palmprint and hand geometry respectively, and generates combined matching score s_c as follows:

$$s_c = \max\{s_p, s_{hg}\} \tag{11}$$

The combined matching score s_c from the two modalities is used for the assign class labels, genuine or imposter, to each of the users.

5. Experiments and results

The experiments reported in this paper utilize inkless hand images obtained from a digital camera, as discussed in Section 2. We collected 1000 images of the left hand, 10 samples from each user, for 100 users. The first five images from each user were used for training and the rest were used for testing. The palmprint images, of size 300×300 pixels, were automatically extracted as described in Section 2.2. Each of the palmprint images was divided into 144 overlapping blocks of size 24×24 pixels, with an overlap of 6 pixels (25%). Thus, a 1×144 feature vector was obtained from every palmprint image. A total of 500 (100×5) genuine and 49,500 ($100 \times 99 \times 5$) imposter matching scores were generated from the test data. Fig. 6 shows the distribution of imposter and genuine matching scores using palmprint and hand geometry features. These two matching scores can be reasonably well separated by a linear discriminant function. The receiver operating characteristic curves for three distinct cases, (i) hand geometry alone, (ii) palmprint alone, and (iii) using matching score level fusion with max rule, i.e., choosing the highest of the similarity measure from hand geometry or palmprint, are shown in Fig. 7.

Some users failed to touch their palm/fingers on the imaging board. It was difficult to use such images, mainly due to a change in image scale and, therefore, these images were later marked as of poor quality. A total of 28 such images were identified and removed. Some of such poor quality images are shown in Fig. 8. The FAR and FRR scores for the remaining 472 test images, using the total

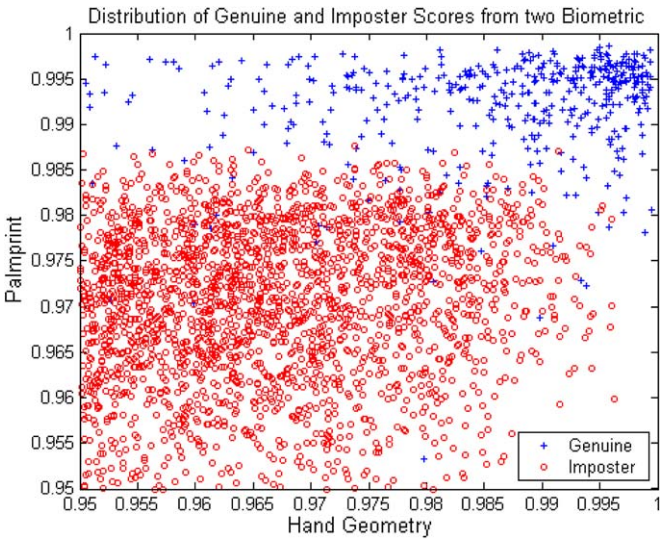

Fig. 6. Distribution of genuine and imposter scores from the two biometric.

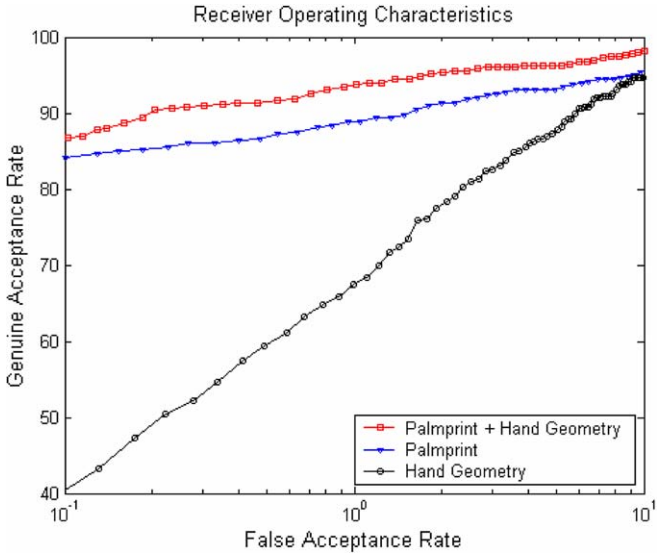

Fig. 7. Comparative performance of palmprint and hand geometry features (500 images) using matching score level fusion.

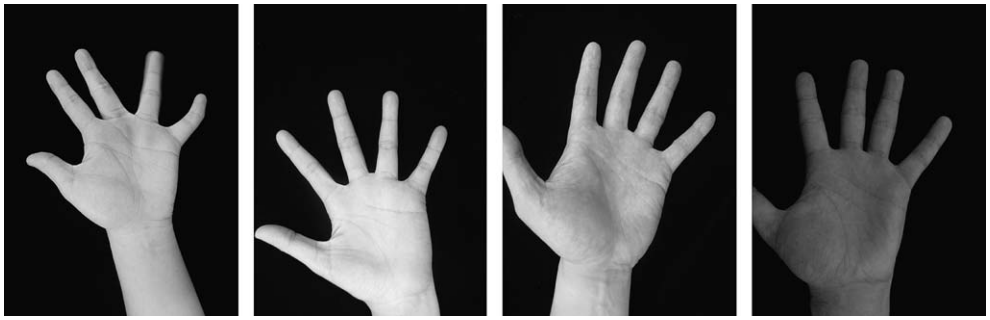

Fig. 8. Samples of poor quality hand images in our database.

Table 1
Performance scores for total minimum error on 472 test images

	FAR (%)	FRR (%)	Decision threshold
Palmprint	4.49	2.04	0.9830
Hand geometry	5.29	8.34	0.9314
Fusion at representation	3.74	1.91	0.9853
Fusion at matching score	0	1.41	0.9840

minimum error as the performance criterion, i.e., the decision threshold at which the sum of FAR and FRR scores is minimum, is shown in Table 1. This table also shows the FAR and FRR scores for each of the biometric at the total minimum error decision threshold. The comparative performance of the two fusion schemes is displayed in Fig. 9. The cumulative distribution of the combined matching scores for the two classes, using matching score level fusion (max rule), is shown in Fig. 10.

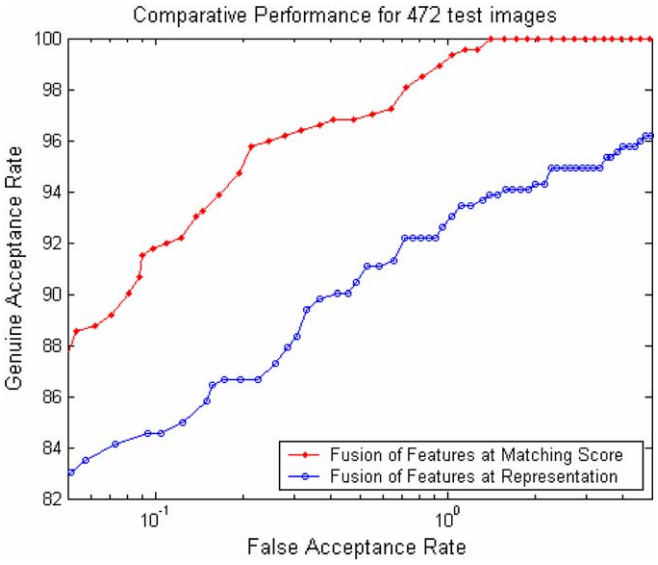

Fig. 9. Comparative performance of two fusion schemes on 472 test images.

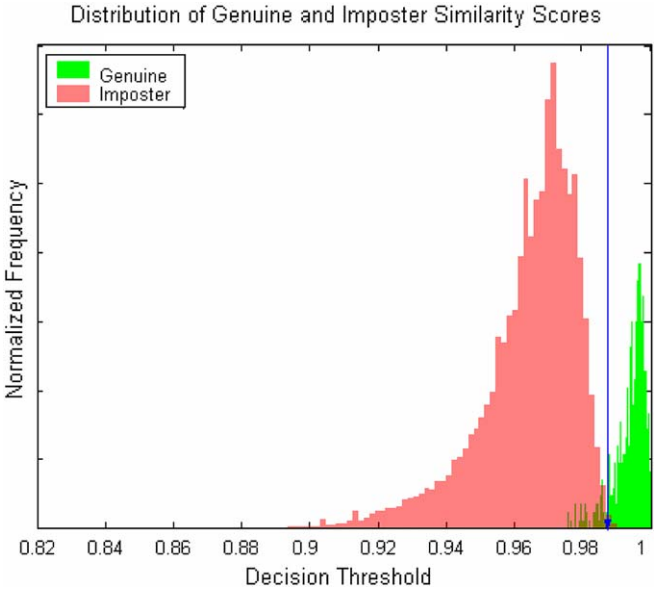

Fig. 10. Distribution of two classes of matching scores for 472 test images.

6. Conclusions

The objective of this work was to investigate the integration of palmprint and hand geometry features, and to achieve a better performance that may not be achievable with single biometric indicator alone. The results obtained in Fig. 7, from 100 users, demonstrate that this is indeed the case. These results should be interpreted in the context of a rather simple image acquisition setup and a small database; further improvement in performance, in the presence of controlled illumination/environment, is intuitively expected. The method described in this work is completely automated, inherently simple and tailored for its practical usage. The achieved results are significant since the two biometric traits were derived from the same image, unlike other bimodal biometric systems which require two different sensors/images. Our results also show that the matching score level fusion scheme, with max rule, achieves better performance than those with fusion at the representation level. The hand geometry based authentication systems offer least user transaction time (Mansfield et al., 2001) which is the key factor in their higher user-acceptance. The method presented in this paper can be used to enhance the performance of existing hand geometry based systems without compromising on the transaction time since both the biometrics (hand shape and palmprint) are acquired simultaneously.

References

Baskan, S., Balut, M.M., Atalay, V., 2002. Projection based method for segmentation of human face and its evaluation. Pattern Recognition Lett. 23, 1623–1629.

Ben-Yacoub, S., Abdeljaoued, Y., Mayoraz, E., 1999. Fusion of face and speech data for person identity verification. IEEE Trans. Neural Networks 10, 1065–1074.

Chen, J., Zhang, C., Rong, G., 2001. Palmprint recognition using crease. In: Proc. Internat. Conf. on Image Process., October 2001, pp. 234–237.

Duta, N., Jain, A.K., Mardia, Kanti V., 2002. Matching of palmprint. Pattern Recognition Lett. 23 (4), 477–485.

Ernst, R.H., 1971. Hand ID system. US Patent No. 3576537.

Funada, J., Ohta, N., Mizoguchi, M., Temma, T., Nakanishi, K., Murai, A., Sugiuchi, T., Wakabayashi, T., Yamada, Y., 1998. Feature extraction method for palmprint considering elimination of creases. In: Proc. 14th Internat Conf. Pattern Recognition, vol. 2, August 1998, pp. 1849–1854.

Gunther, M., 2002. Device for identifying individual people by utilizing the geometry of their hands. European Patent No. DE10113929.

Han, C.-C., Jang, B.-J., Shiu, C.-J., Shiu, K.-H., Jou, G.-S., 2002. Hand features verification system of creatures. European Patent No. TW476917.

Han, C.-C., Cheng, H.-L., Lin, C.-L., Fan, K.-C., 2003. Personal authentication using palm-print features. Pattern Recognition 36, 371–381.

Haralick, R.M., Shapiro, L.G., 1991. Computer Vision and Robot Vision, vol. I. Addison-Wesley.

Hong, L., Jain, A.K., 1998. Integrating face and fingerprint for personal identification. IEEE Trans. Pattern Anal. Machine Intell. 20 (Dec), 1295–1307.

Jacoby, I.H., Giordano, A.J., Fioretti, W.H., 1972. Personal identification apparatus. US Patent No. 3648240.

Jain, A.K., Bolle, R., Pankanti, S., 1999. Biometrics: Personal Identification in Networked Society. Kluwer Academic.

Jain, A.K. Ross, A., Pankarti, S., 1999. A prototype hand geometry based verification system. In: Proc. 2nd Internat. Conf. on Audio Video based Biometric Personal Authentication, March 1999, pp. 166–171.

Joshi, D.G., Rao, Y.V., Kar, S., Kumar, V., 1998. Computer vision based approach to personal identification using finger crease pattern. Pattern Recognition 31 (1), 15–22.

Kittler J., Messer, M., 2002. Fusion of multiple experts in multimodal biometric personal identity verification systems. In: Proc. 12th IEEE Workshop Neural Networks, Guildford (UK), pp. 3–12.

Kittler, J., Hatef, M., Duin, R.P.W., Matas, J., 1998. On combining classifiers. IEEE Trans. Pattern Anal. Machine Intell. 20, 226–239.

Kumar, A., Shen, H.C., 2002. Recognition of palmprints using wavelet-based features. In: Proc. Internat. Conf. on Sys., Cybern., SCI-2002, Orlando, Florida, July.

Kumar, A., Shen, H.C., 2004. Palmprint identification using PalmCodes. In: Proc. 3rd Internat. Conf. on Image & Graphics, ICIG 2004, Hong Kong, December 18–20, pp. 258–261.

Kumar, A., Zhang, D., 2005. Personal authentication using multiple palmprint representation. Pattern Recognition 38, 1695–1704.

Kumar, A., Wong, D.C.M., Shen, H.C., Jain, A.K., 2003. Personal verification using palmprint and hand geometry biometric. In: Proc. AVBPA 2003, Guildford, UK, pp. 668–675.

Kung, S.Y., Lin, S.H., Fang, M., 1995. A neural network based approach to face/palm recognition. In: Proc. Internat. Conf. on Neural Networks, pp. 323–332.

Li, W., Zhang, D., Xu, Z., 2002. Palmprint identification by Fourier transform. Int. J. Pattern Recognition Art. Intell. 16 (4), 417–432.

Mansfield, T., Kelly, G., Chandler, D., Kane, J., 2001. Biometrics Product Testing Final Report, Computing, National Physical Laboratory, Crown Copyright, UK. Available from: <http://www.cesg.gov.uk/site/ast>.

Miller, R.P., 1971. Finger dimension comparison identification system. US Patent No. 3576538.

Oden, C., Ercil, A., Buke, B., 2003. Combining implicit polynomials and geometric features for hand recognition. Pattern Recognition Lett. 24, 2145–2152.

Otsu, N., 1978. A threshold selection method from gray-scale histogram. IEEE Trans. Systems Man Cyberner. 8, 62–66.

Prabhakar, S., Jain, A.K., 2002. Decision level fusion in fingerprint verification. Pattern Recognition 35, 861–874.

Prabhakar, S., Jain, A.K., Pankanti, S., 2003. Learning fingerprint location and type. Pattern Recognition 36, 1847–1857.

Sanchez-Reillo, R., Sanchez-Avila, C., Gonzales-Marcos, A., 2000. Biometric identification through hand geometry measurements. IEEE Trans. Pattern Anal. Machine Intell. 22 (10), 1168–1171.

Sidlauskas, D.P., 1988. 3D hand profile identification apparatus. US Patent No. 4736203.

Wu, X., Wang, K., Zhang, D., 2002. Fuzzy directional energy element based palmprint identification. In: Proc. ICPR-2002, Quebec City, Canada, pp. 95–98.

Yang, M.-H., Kriegman, D.J., Ahuja, N., 2002. Detecting faces in images: A survey. IEEE Trans. Pattern Anal. Machine Intell. 24 (Jan), 34–58.

You, J., Li, W., Zhang, D., 2002. Hierarchical palmprint identification via multiple feature extraction. Pattern Recognition 35, 847–859.

Zhang, D., Shu, W., 1999. Two novel characteristics in palmprint verification: Datum point invariance and line feature matching. Pattern Recognition 32 (4), 691–702.